Short Abstract for 2004 AAS/AIAA Space Flight Mechanics Meeting,
Maui, Hawaii, Feb. 8-12, 2004

Modeling of Proof Mass Self-Gravity Field for the Laser Interferometry Space Antenna (LISA)[1]

Dr. Marco B. Quadrelli
M.S. 198-326
Jet Propulsion Laboratory
California Institute of Technology
4800 Oak Grove Drive
Pasadena, CA 91109
marco@grover.jpl.nasa.gov

This paper describes the development of the self-gravity modeling tool used to predict and control the motion of one of the proof masses of the orbiting LISA gravitational wave detector. LISA is a space-borne gravitational wave detector, which is formed by three spacecraft orbiting the Sun and forming the vertices of an equilateral triangle with a side of 5 million km in length. Requirements on the forces and moments, and the force gradients and moment gradients, applied to the proof mass exist. This paper computes these quantities analytically, so that gravitational balancing considerations can now be done effectively.

[1] This research was performed at the Jet Propulsion Laboratory, California Institute of Technology, under contract with the National Aeronautics and Space Administration.

Extended Abstract for 2004 AAS/AIAA Space Flight Mechanics Meeting,
Maui, Hawaii, Feb. 8-12, 2004

Modeling of Proof Mass Self-Gravity Field for the Laser Interferometry Space Antenna (LISA)[2]

Dr. Marco B. Quadrelli
M.S. 198-326
Jet Propulsion Laboratory
California Institute of Technology
4800 Oak Grove Drive
Pasadena, CA 91109
marco@grover.jpl.nasa.gov

This paper describes the development of the self-gravity tool used to predict and control the motion of one of the proof masses of the orbiting LISA gravitational wave detector. LISA is a space-borne gravitational wave detector, which is formed by three spacecraft orbiting the Sun and forming the vertices of an equilateral triangle with a side of 5 million km in length. Inside each spacecraft, shown in Figure 1, an optical bench monitors the motion of two separated proof masses, which reflect the laser light from the adjacent spacecraft along the edges of the equilateral triangle, and senses the gravitational wave signal with unprecedented sensitivity.

The paper describes the details of the self-gravity tool developed at JPL and used for gravitational balancing of the spacecraft. A modeling challenge described in the paper is how to consider the distributed force and torque between all the participating extended bodies. Gravitational forces and moments on each extended body are computed exactly from the closed form expression of the gravitational potential of a parallelepiped. This approach is currently being incorporated into a general finite element-based self-gravity computational tool at JPL for the LISA spacecraft. Requirements on the forces and moments, and the force gradients and moment gradients, applied to the proof mass exist, therefore these quantities must be computed independently.

Figure 2 depicts the geometry of the problem, and the potential of the gravitational interaction between an extended three-dimensional parallelopiped and a point mass source, located at x. Here, the proof mass, or a sub-element of it shaped as a parallelepiped, interacts gravitationally with the point source mass M. Any arbitrary mass distribution surrounding the proof mass can be thus computed by combining the effects of each point mass individually. Denote the distance between these two mass elements by ***r***, so that ***r*** represents the distance between the origins of the two extended bodies "proof mass" and "source body M". The gravitational potential due to the interaction is

[2] This research was performed at the Jet Propulsion Laboratory, California Institute of Technology, under contract with the National Aeronautics and Space Administration.

$$V = V(\mathbf{r}) = GMm|\mathbf{r}|^{-1}$$

Let us vary the kinematics of the parallelepiped B, keeping the source M fixed, and assuming only small rotations:

$$\delta\mathbf{r} = -\delta^o\mathbf{r} + (\mathbf{r}\times 1)\cdot\delta\boldsymbol{\theta}$$

then the virtual variation of the potential becomes:

$$\delta V = \frac{\partial V}{\partial\mathbf{r}}\cdot\delta^0\mathbf{r} + \left(\mathbf{r}\times\frac{\partial V}{\partial\mathbf{r}}\right)\cdot\delta\boldsymbol{\theta}$$

Consequently, the forces and moments, and the forces and moment gradients originate from the variation of the potential as follows:

$$F = \frac{\partial V}{\partial\mathbf{r}}$$

$$M = \mathbf{r}\times\frac{\partial V}{\partial\mathbf{r}}$$

$$\begin{pmatrix}\delta\mathbf{F}\\ \delta\mathbf{M}\end{pmatrix} = \begin{bmatrix}\dfrac{\partial V}{\partial^0\mathbf{r}\partial^0\mathbf{r}} & \mathbf{r}\times\dfrac{\partial V}{\partial^0\mathbf{r}\partial^0\mathbf{r}}\\ \dfrac{\partial\mathbf{M}}{\partial(\partial^o\mathbf{r})} & \dfrac{\partial\mathbf{M}}{\partial(\partial\boldsymbol{\theta})}\end{bmatrix}\begin{pmatrix}\delta^0\mathbf{r}\\ \delta\boldsymbol{\theta}\end{pmatrix}$$

$$\frac{\partial\mathbf{M}}{\partial(\partial^o\mathbf{r})} = \mathbf{E}_1 - \mathbf{F}\times\mathbf{U}$$

$$\frac{\partial\mathbf{M}}{\partial(\partial\boldsymbol{\theta})} = (\mathbf{r}\otimes\mathbf{F}) - (\mathbf{F}\cdot\mathbf{r})\mathbf{U} - \mathbf{E}_2$$

where the symbol $\otimes$ represents outer product, and with the following definitions:

$$\mathbf{r}\times\left(\frac{\partial F}{\partial^o\mathbf{r}}\cdot\partial^o\mathbf{r}\right) = \mathbf{E}_1\partial^o\mathbf{r}$$

$$\mathbf{r}\times\left[\frac{\partial F}{\partial^o\mathbf{r}}\cdot(\mathbf{r}\times\partial\boldsymbol{\theta})\right] = \mathbf{E}_2\partial\boldsymbol{\theta}$$

The last step is to sum over all points $\mathbf{x}$ of any extended body around the proof mass parallelepiped. This can be done either by summing over a (very) large number of points, or by integrating over finite elements of irregular shapes at the Gauss-Legendre nodes.

Figure 3 shows the computed bounds below which one can consider an adjacent extended body as a point mass with respect to the proof mass. Figure 4 shows the initial mesh used for predicting the gravitational interaction between two extended cubes. The methods used for modeling the gravitational field and its gradients are: 1) by summing the gravitational forces and gradients after discretization of the source mass into a large number of mass points, (Figure 5), and 2) by summing the gravitational forces and gradients after discretization of the source mass into a much smaller number of Gauss-Legendre points (Figure 6). The conclusion is that very few, optimally located Gauss-Legendre points (4 points along each side of the cube, in the example of Figure 3) achieve the same result (accuracy of force prediction within 0.5% of exact value) than more that 5000 points into which the source cube is discretized. This result is extremely convenient for analyses using a dynamic gravitational field, and gravitational balancing considerations can now be done effectively. A second paper applies some of these models to the gravitational dynamic control of the displacement of the proof mass.

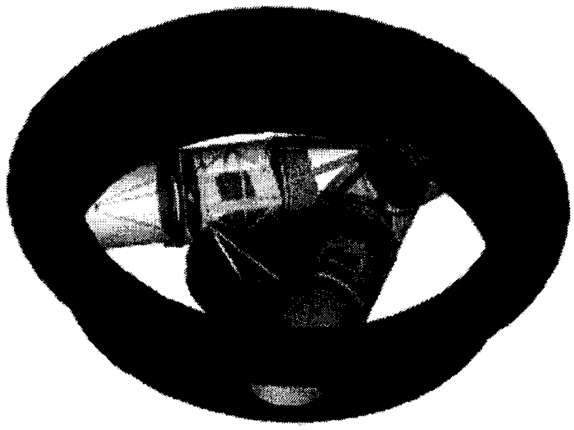

Figure 1. Picture of LISA spacecraft.

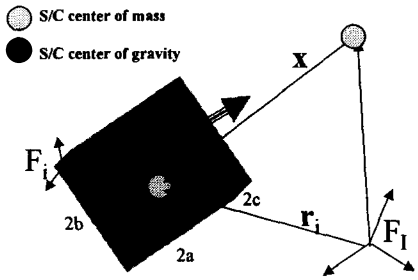


```
Vaa(1) =+(x1+a)*(x2+b)*log((r1+r2+2*c)/(r1+r2-2*c));
Vaa(2) =-(x1+a)*(x2-b)*log((r3+r4+2*c)/(r3+r4-2*c));
Vaa(3) =+(x1+a)*(x3+c)*log((r1+r3+2*b)/(r1+r3-2*b));
Vaa(4) =-(x1+a)*(x3-c)*log((r2+r4+2*b)/(r2+r4-2*b));
Vaa(5) =+(x1-a)*(x2-b)*log((r7+r8+2*c)/(r7+r8-2*c));
Vaa(6) =-(x1-a)*(x2+b)*log((r5+r6+2*c)/(r5+r6-2*c));
Vaa(7) =+(x1-a)*(x3-c)*log((r6+r8+2*b)/(r6+r8-2*b));
Vaa(8) =-(x1-a)*(x3+c)*log((r5+r7+2*b)/(r5+r7-2*b));
Vaa(9) =+(x2+b)*(x3+c)*log((r1+r5+2*a)/(r1+r5-2*a));
Vaa(10)=-(x2+b)*(x3-c)*log((r2+r6+2*a)/(r2+r6-2*a));
Vaa(11)=+(x2-b)*(x3-c)*log((r4+r8+2*a)/(r4+r8-2*a));
Vaa(12)=-(x2-b)*(x3+c)*log((r3+r7+2*a)/(r3+r7-2*a));
Va=sum(Vaa);
```

```
Vbb(1)=atan((x2+b)*(x3-c)/((x1+a)*r2))-...
       atan((x2+b)*(x3+c)/((x1+a)*r1))+...
       atan((x2-b)*(x3+c)/((x1+a)*r3))-...
       atan((x2-b)*(x3-c)/((x1+a)*r4));
Vbb(2)=atan((x2+b)*(x3+c)/((x1-a)*r5))-...
       atan((x2+b)*(x3-c)/((x1-a)*r6))+...
       atan((x2-b)*(x3-c)/((x1-a)*r8))-...
       atan((x2-b)*(x3+c)/((x1-a)*r7));
Vbb(3)=atan((x1-a)*(x3+c)/((x2+b)*r5))-...
       atan((x1+a)*(x3+c)/((x2+b)*r1))+...
       atan((x1+a)*(x3-c)/((x2+b)*r2))-...
       atan((x1-a)*(x3-c)/((x2+b)*r6));
Vbb(4)=atan((x1+a)*(x3+c)/((x2-b)*r3))-...
       atan((x1-a)*(x3+c)/((x2-b)*r7))+...
       atan((x1-a)*(x3-c)/((x2-b)*r8))-...
       atan((x1+a)*(x3-c)/((x2-b)*r4));
Vbb(5)=atan((x1+a)*(x2-b)/((x3+c)*r3))-...
       atan((x1+a)*(x2+b)/((x3+c)*r1))+...
       atan((x1-a)*(x2+b)/((x3+c)*r5))-...
       atan((x1-a)*(x2-b)/((x3+c)*r7));
Vbb(6)=atan((x1+a)*(x2+b)/((x3-c)*r2))-...
       atan((x1+a)*(x2-b)/((x3-c)*r4))+...
       atan((x1-a)*(x2-b)/((x3-c)*r8))-...
       atan((x1-a)*(x2+b)/((x3-c)*r6));
Vb=0.5*((x1+a)^2)*Vbb(1)+...
   0.5*((x1-a)^2)*Vbb(2)+...
   0.5*((x2+b)^2)*Vbb(3)+...
   0.5*((x2-b)^2)*Vbb(4)+...
   0.5*((x3+c)^2)*Vbb(5)+...
   0.5*((x3-c)^2)*Vbb(6);
```

Potential V=Va+Vb

Figure 2. Gravitational potential of parallelopiped due to a gravitational point source at x.

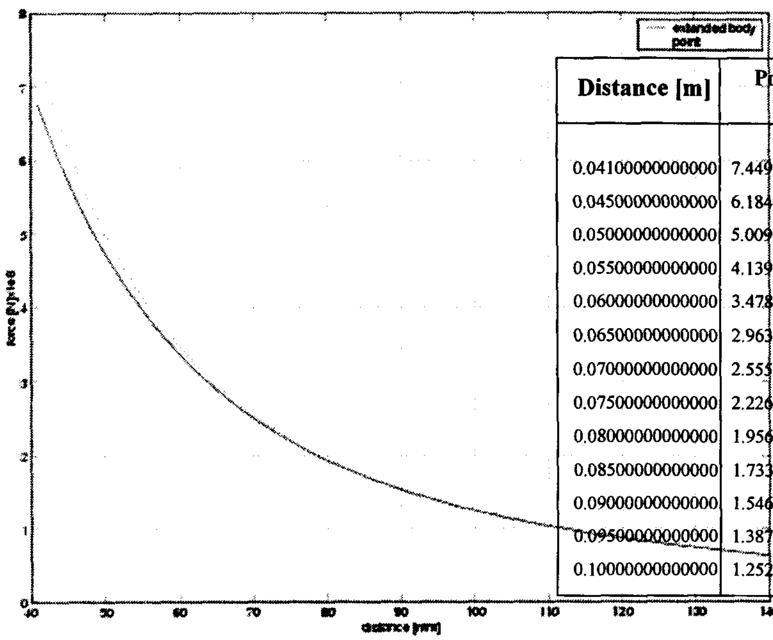

Distance [m]	Point mesh	Extended body mesh
0.04100000000000	7.44954003569304	6.77484428853350
0.04500000000000	6.18403792592593	5.73742236550000
0.05000000000000	5.00907072000000	4.73625787810724
0.05500000000000	4.13972786776860	3.96931811286107
0.06000000000000	3.47852133333333	3.36959796207972
0.06500000000000	2.96394717159763	2.89271808285454
0.07000000000000	2.55564832653061	2.50803441655495
0.07500000000000	2.22625365333333	2.19375709541000
0.08000000000000	1.95666825000000	1.93405352102910
0.08500000000000	1.73324246366782	1.71721726971168
0.09000000000000	1.54600948148148	1.53446185729754
0.09500000000000	1.38755421606648	1.37910323126386
0.10000000000000	1.25226768000000	1.24599386243872

Figure 3. Bounds for considering adjacent masses as points.

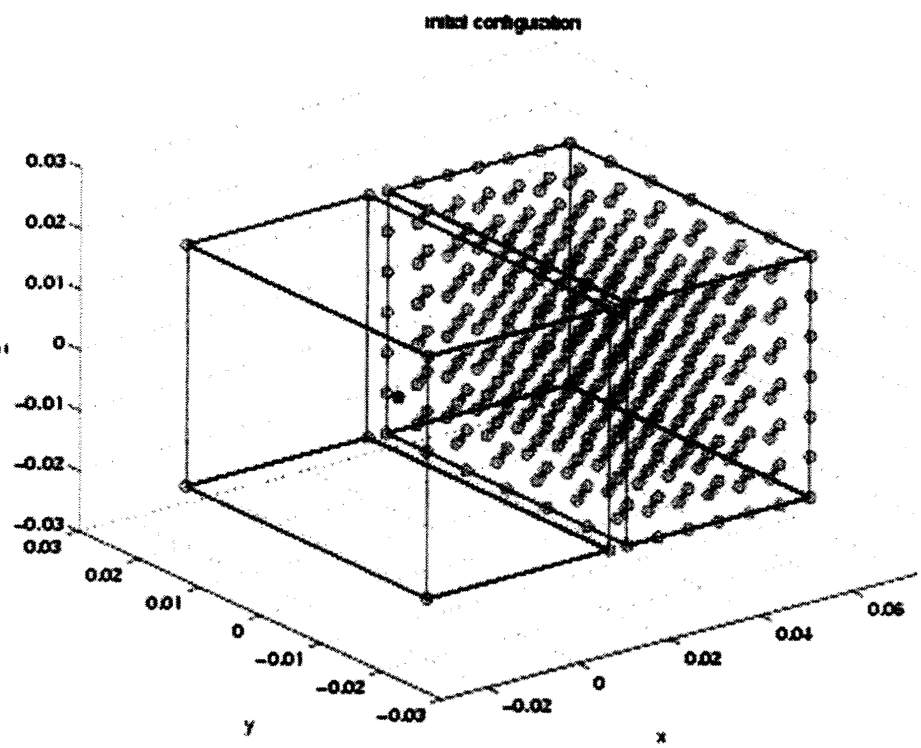

Figure 4. Two cube problem.

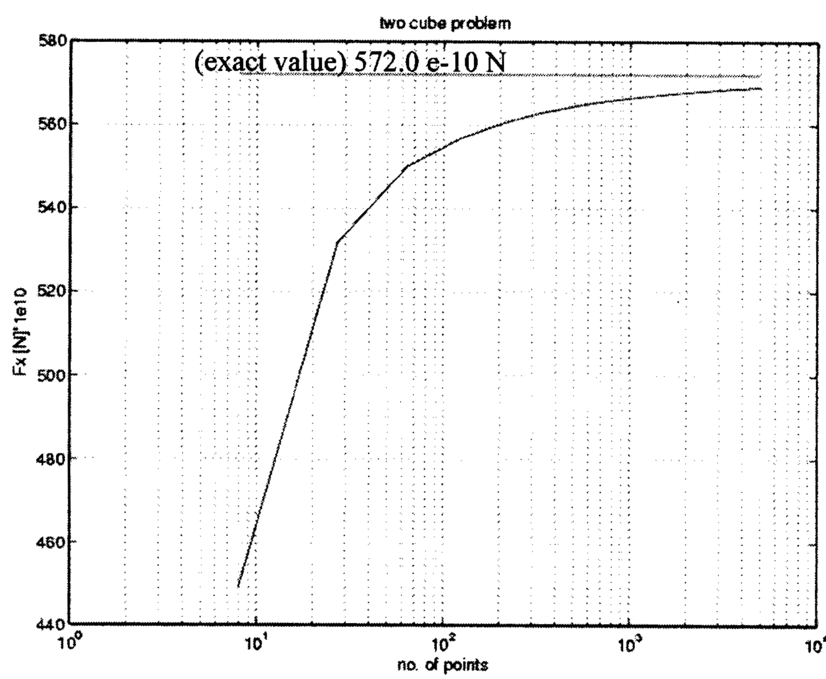

Figure 5. Axial force in two cube problem as a function of discretization points.

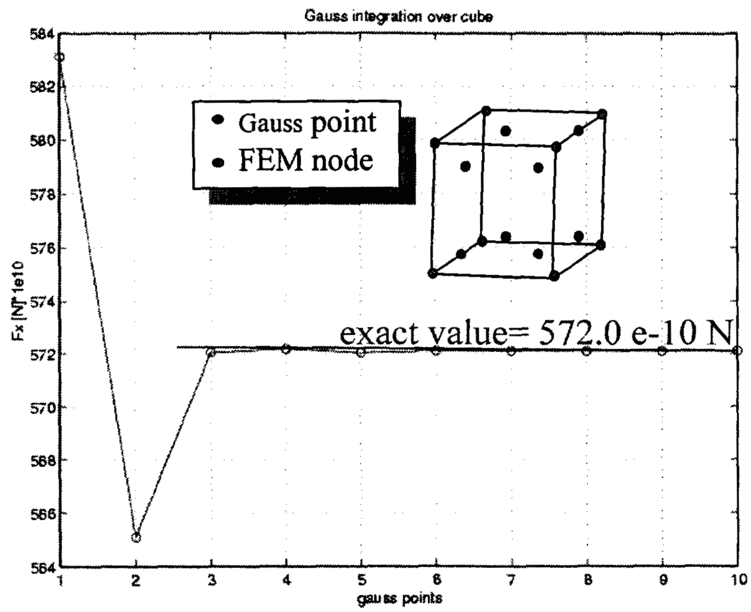

Figure 6. Axial force in two cube problem as a function of Gauss quadrature points.